



Development of solvent regeneration process

N.K. Pandey*, R. Rajeev, C.V. Joyakin, P. Vishnu Anand, P. Velavendan,
U. Kamachi Mudali, R. Natarajan

RR and DD, Reprocessing Group, Indira Gandhi Centre for Atomic Research, Kalpakkam, Tamil Nadu 603102, India

Tel. +91 44 274 80126; Fax: +91 44 274 80126; email: nkpandey@igcar.gov.in

Received 4 February 2012; Accepted 16 July 2013

ABSTRACT

The useful life of the hydrocarbon-tri-butyl phosphate solvent system in nuclear fuel reprocessing plant is limited by the extent of formation of secondary degradation compounds. These are formed by the interaction of nitric and nitrous acids with the various hydrocarbon compounds under the conditions of radiation. One of the easily deployable methods for the removal of these degradation products (secondary degradation products) is distillation. The instability of tri-*n*-butyl phosphate at elevated temperatures and the requirement that very low concentrations of variety of impurities that have to be removed call for a careful design of process and equipment. A pilot plant scale solvent purification system based on vacuum distillation has been designed, developed, and commissioned at the Reprocessing Development Laboratory, Indira Gandhi Centre for Atomic Research. The solvent recovery system is an integration of different liquid–vapor separation units such as dehydration column, agitated thin film evaporator, and vacuum-distillation column. The performances of the auxiliary equipment were monitored by conducting trial runs with simulated degraded solvent. The results obtained from the trial runs were analyzed by measuring the physical and extraction properties.

Keywords: Solvent regeneration; Fuel reprocessing; Vacuum distillation; PUREX process

1. Introduction

Reprocessing of spent nuclear fuel is indispensable for the economic use of uranium in nuclear energy production and has been used industrially for more than five decades. These processes involve the use of an extractant and a diluent for the separation of the reusable actinides from the unwanted fission products. The most widely used PUREX process [1] employs tributyl phosphate (TBP) as the extractant diluted with a hydrocarbon. It is widely recognized

that TBP and hydrocarbon diluents are degraded due to hydrolytic and radiolytic reactions, forming activity-binding degradation products that can cause product losses, poor separation efficiencies and emulsions which could interfere with process operations. The primary degradation products (i.e. dibutyl phosphate, monobutyl phosphate, phosphoric acid, and butanol) are produced from the hydrolytic and dealkylation reactions of the TBP when contacted with nitric acid at relatively high temperatures. The secondary degradation products (nitroparaffins, aldehydes, ketones, and carboxylic acids), on the other hand, are

*Corresponding author.

originated from the radiolytic reactions of diluents when exposed to intensive radiation [2–5]. In the Purex process, the spent solvent is continuously regenerated by scrubbing with sodium carbonate/hydroxide after each pass through the process and most of the radioactivity belonging to primary degradation products is removed. Residual activity due to secondary degradation products, however, cannot be removed by washing these solutions as the degraded long-chain soluble organic compounds tend to remain in the solvent even after scrubbing with carbonate washing solutions and complex fission products again when the solvent is recycled. These degradation products progressively accumulate in the solvent with repeated recycling and their removal from the solvent is not well addressed as that of the primary degradation products of TBP. With time, the solvent performance characteristics become so impaired that its partial refreshment is required at intervals. In fact, the amount of organics generated in the extraction process can be reduced considerably by adopting a suitable solvent regeneration process. A common method for their removal is distillation. The instability of tri-*n*-butyl phosphate at elevated temperature requires the evaporator and distillation columns to be operated at reduced temperature to avoid thermal degradation of solvent which calls for operation at reduced pressure. Though considerable effort has been devoted for the development of this method for solvent purification [6–11], its industrial application is limited [12].

A pilot plant scale solvent purification system based on vacuum distillation has been designed, developed, and commissioned at the Reprocessing Development Laboratory, of Indira Gandhi Centre for Atomic Research, by the authors of the present work. The performances of process and auxiliary equipment were monitored by conducting trial runs with simulated degraded solvent. The results obtained from the initial runs were analyzed by measuring the physical and extraction properties and are reported in this paper.

2. Process description

The photograph of the solvent purification plant (throughput ~15 LPH) developed based on vacuum distillation is shown in Fig. 1. The solvent recovery system is an integration of different liquid–vapor separation units such as dehydrator, wiped film evaporator, and distillation column.

The flow diagram of solvent purification process is depicted in Fig. 2. The spent solvent (degraded solvent) was first given an alkali wash to remove primary degradation products of TBP (such as DBP



Fig. 1. Pilot plant solvent purification system.

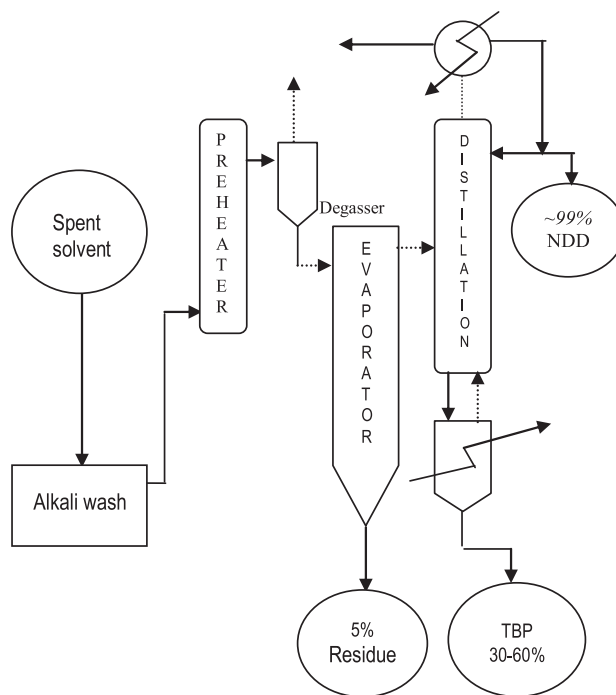


Fig. 2. Process flow diagram of solvent purification system.

and MBP) and then passed through a dehydration column (preheater) in which water is evaporated.

Necessity of dehydration column arises from the fact that water will behave as noncondensable vapor in the condenser of the main distillation unit owing to low operating pressure of 1 torr. Dehydration was performed under reduced pressure (~30 torr) in a counter current evaporator. The solvent containing degraded products was then passed through a wiped film evaporator, where solvent was evaporated to the level of 95% and the 5% residue containing all the heavy compounds (degradation products of solvent and diluent) was discarded as waste product. The solvent vapor was then passed into a rectification column, where diluents of about 99% purity as top product and the bottom product of 40–70% TBP were obtained.

3. Design aspects

The basic design of purification process is based on the design of falling/wiped film evaporator and distillation column, which are operated at 10 and 1 torr, respectively. Design calculations were performed for associated heat transfer equipment for the estimation of heat transfer area. Physical properties used in the design calculations are listed in Table 1.

3.1. Preheater

Function of the preheater is to remove moisture from feed solvent as water vapor behaves like noncondensable in the condenser of distillation column, which reduces the performance of the condenser. It is a shell and tube heat exchanger with feed on tube side and heating medium on shell side. All contact parts are made of SS 304L and noncontact parts are of carbon steel. Standard design equations for shell and tube heat exchanger were used for the determination of required heat transfer area.

3.2. Degasser

This is a packed column with structured packing with de-entrainment section for liquid–vapor separation. Material of construction is SS 304L.

Vapor pressure (P_{TBP}) of TBP is given by:

$$P_{TBP} = \left(\frac{760}{1.01333 \times 10^5} \right) \exp \left(A - \frac{B}{T} - \frac{C}{T^2} \right) \quad (1)$$

where P_{TBP} is in mm Hg; T : temperature, K; $A = 17.715$; $B = 981.49$; $C = 1.4583 \times 10^6$.

Vapor pressure (P_{NDD}) of NDD is given by:

$$P_{NDD} = 10^n$$

where P_{NDD} is in mm Hg and T is temperature in K.

$$n = A + \frac{B}{T} + C \log_{10} T + D \times T + E \times T^2 \quad (2)$$

$$A = -5.6532; \quad B = -3.4698 \times 10^3; \quad C = 9.0272; \\ D = -2.3185 \times 10^{-2}; \quad E = 1.1235 \times 10^{-5}.$$

3.3. Agitated thin film evaporator

Agitated thin film evaporator (ATFE) is widely used in chemical, pharmaceutical, and food industries. The combination of short residence time, high turbulence, and rapid surface renewal permits the ATFE to successfully handle heat sensitive, viscous, and fouling feed stream. The main reason to use ATFE is to obtain a high heat transfer coefficient (about 700–800 W/m²K) [13] for the process side fluid that would not be possible in a conventional evaporator.

When this type of equipment seems to be right choice in a given situation, the common approach is to ask a vendor and conduct an evaluation and get a

Table 1
Physical properties of TBP–NDD system

Parameter	TBP	NDD
Density (kg/m ³) [where T is in °C]	$\rho_{TBP} = 994.21 - 0.8517T$	$\rho_{NDD} = 776.29 - 0.7588T$
Viscosity (cp) [where T is in °C]	$\mu_{TBP} = \exp \left(-3.239 + \frac{844.758}{164.854 + T} \right)$	$\mu_{NDD} = \exp \left(-4.199 + \frac{1191.697}{250.538 + T} \right)$
Specific heat J/(g °C)	$C_{PTBP} = 1.7685 + 2.1125 \times 10^{-3} + 2.365 \times 10^{-6} T^2$	$C_{PNDD} = 1.9598 + 5.3315 \times 10^{-3} - 6.79 \times 10^{-6} T^2$
Surface tension (mN/m)	$\sigma_{TBP} = 30.33 - 0.0988T$	$\sigma_{NDD} = 25.16 - 0.0853T$
Diffusivity (cm ² /s)	$D_{TBP} = 7.69 \times 10^{-9} T$, where T is in K	Not known
Latent heat of vaporization (J/kg)	$\lambda_{TBP} = 15,945 \times \sqrt{512 - T}$ where T is in °C	$\lambda_{NDD} = 18,581 \times \sqrt{387.2 - T}$ where T is in °C

quote for this type of equipment. The quality of such an evaluation depends upon the data that the manufacturer receives from the potential user. ATFEs are commercially available in various configurations and it was supplied to us by M/s Shefa Engineers, Ghaziabad, Delhi, based on the input data provided by the authors of this work.

The ATFE consists of two major assemblies: a heated body (cylindrical shell) and a close clearance rotor. The cylindrical shell is machined from inside to close tolerances and has jacketed section for hot oil heating. The shell is 0.15 m in diameter and 0.5 m long, providing heat transfer area of about 0.2 m². The rotor is multi-bladed, dynamically balanced, and attached to the drive motor shaft through a mechanical seal suitable for vacuum service. The process fluid enters the unit tangentially above the heated zone and distributes evenly over the inner surface of the shell wall by rotating action of rotor blade. The blades of rotor spread the liquid over the entire heated wall and generate highly turbulent flow conditions.

Thermal design of ATFE is similar to the conventional heat exchanger wherein the first step is to obtain the overall heat transfer coefficient and then calculate the desired heat transfer area for a given capacity. The amount of heat transferred from hot fluid to process fluid is related by,

$$Q = UA\Delta T_{lm} = m C_{ph}(T_{hi} - T_{ho}) \quad (3)$$

where Q , the heat duty, is fixed by process requirement; U , the overall heat coefficient, depends on the physical properties of process fluid and heating medium; A is the heat transfer area; and ΔT_{lm} is the logarithmic mean temperature difference. Further, m , C_{ph} , T_{hi} , and T_{ho} are the mass flow rate, heat capacity, and hot fluid inlet and outlet temperature, respectively.

Overall heat transfer coefficient (U) can be expressed in terms of individual heat transfer coefficients for heating medium and process fluid side. Referring Fig. 3, U can be written as:

$$\frac{1}{U} = \frac{1}{h_h} + \frac{1}{h_p} \quad (4)$$

where h_h is the jacket-side heat transfer coefficient and h_p is the process-side heat transfer coefficient. The jacket-side heat transfer coefficient is determined by using the following well-known Dittus–Boelter equation:

$$Nu = 0.023 Re^{0.8} Pr^{0.4} \quad (5)$$

where the Reynolds number and Prandtl number are given by,

$$Re = \frac{D_e u_h \rho_h}{\mu_h}$$

$$Pr = \frac{C_{ph} \mu_h}{K_h}$$

The equivalent diameter (D_e) for the annulus is given by,

$$D_e = D_o - D_i \quad (6)$$

The jacket-side heat transfer coefficient is

$$h_h = \frac{Nu K_h}{D_e} \quad (7)$$

The wall temperature (T_w) can be calculated from,

$$T_w = T_h - \frac{Q}{h_h A_h} \quad (8)$$

Process fluid-side heat transfer coefficient (h_p) is reported to be a function of the number of blades, the speed of rotation of blades, and the physical properties of process fluid. The expression for h_p is given as follows:

Bott and Romero [14]:

$$Nu = 0.018 Re_f^{0.46} Re_r^{0.6} Pr_L^{0.87} (D/L)^{0.48} N_b^{0.24} \quad (9)$$

Bott and Sheikh [15]:

$$Nu = 0.65 Re_f^{0.25} Re_r^{0.43} Pr_L^{0.3} N_b^{0.33} \quad (10)$$

where D is the diameter, L is the height, N_b is the number of blades, and N is the rotational speed, and the dimensionless numbers are

$Nu = \frac{h_p D}{K}$ is the Nusselt number

$Re_r = \frac{D^2 N \rho_p}{\mu_p}$ is the rotational Reynolds number

$Re_f = \frac{4F}{\pi D \mu}$ is the film Reynolds number

$Pr = \frac{C_{pp} \mu_p}{K_p}$ is the Prandtl number

Considering the ATFE as a stage-wise unit (dividing the length into a number of stages, Fig. 3) the performance of ATFE can be predicted using mass

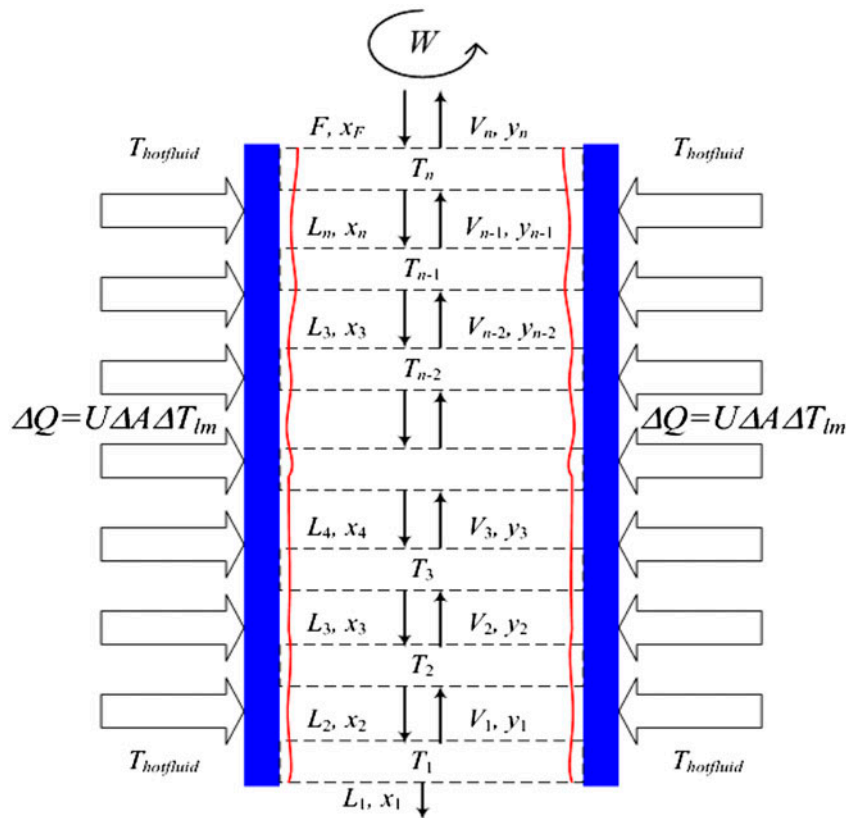


Fig. 3. Representation of ATFE as a stage-wise unit.

balance and energy balance equations. Applying mass balance, energy balance, and equilibrium considerations to the stage, the amount of vapor can be calculated.

Mass balance:

$$L_n + V_n = F + V_{n-1} \quad (11)$$

$$L_n x_n + V_n y_n = F x_f + V_{n-1} y_n \quad (12)$$

Equilibrium:

$$K_n = \frac{y_n}{x_n} \quad (13)$$

Energy balance:

$$L_n h_{L,n} + V_n h_{V,n} = F h_{L,f} + V_{n-1} h_{V,n-1} + \Delta q \quad (14)$$

$$V_{n-1} = \frac{L_n h_{L,n} + V_n h_{V,n} - F h_{L,f} - \Delta q}{h_{V,n-1}} \quad (15)$$

where $\Delta q = U\Delta A\Delta T_{lm}$.

3.4. Distillation column

For the design of distillation column, vapor-liquid equilibrium (VLE) data for TBP-n-dodecane system were generated at 1 and 10 torr vacuum. The number of theoretical stages for the separation of binary mixture of TBP and n-dodecane was estimated by McCabe-Thiele diagram which is shown in Fig. 4. The wide difference in the boiling point between TBP and n-dodecane is advantageous as only two theoretical stages are sufficient enough to achieve desired separation which is obvious from Fig. 4.

Distillation column is a packed tower of 0.2 m in diameter and 2 m in length. SS wire mesh structured packing suitable for low pressure distillation is used. The HETS for this type of packing was provided by the supplier and is about 0.3 m. Considering a maximum of three number of theoretical stages, the height of the distillation column was chosen to be 2 m. The diameter of the column was estimated considering flooding condition. The column is provided with liquid distributor, liquid collector, and packing supports. All contact parts are made of SS 304L.

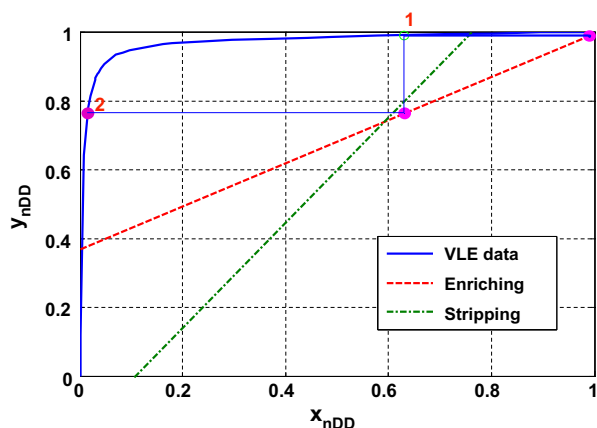


Fig. 4. McCabe Thiele diagram for separation of binary TBP–NDD mixture.

3.5. Condenser

It is a shell and tube-type heat exchanger providing a heat transfer area of 0.25 m^2 and located at the top distillation column. The required heat transfer area was calculated using design equations. Chilled water is supplied through shell side, whereas hot fluid (vapor) passed through the tube side.

3.6. Reboiler

It is a thermo-syphon-type reboiler in shell and tube constructions and providing a heat transfer area of about 0.5 square meters which was estimated by applying overall heat balance and standard heat exchanger design equations using the physical properties data given in Table 1. All contact parts are made with SS 304L and noncontact parts in carbon steel. Reboiler heat load (H_R) was calculated by the following relation:

$$H_R = Q_C + H_{\text{dist}} + H_{\text{Bottom}} - H_{\text{Feed}} \quad (16)$$

where Q_C , H_{dist} , H_{Bottom} , and H_{Feed} are condenser heat load and enthalpy of distillate, bottom product, and feed, respectively, which were calculated using physical property data and their respective flow rates.

4. Experimental and results

In the experimental studies, TBP was diluted with NPH (having the general formula C_nH_{2n+2}) to prepare 30 vol.% TBP. The NPH used was obtained from M/s Reliance Petrochemicals, the chemical composition of which is given Table 2 and it has almost similar physical properties as that of *n*-dodecane. As *n*-dodecane is very expensive, it was used only for VLE data

generation. Several experimental runs were conducted with the simulated solvent (solvent had unidentified degradation products as it was stored for very long period after it was equilibrated with HNO_3) to optimize the operating parameters and evaluate the quality of products from the distillation column. Table 3 lists the operating conditions of various equipment of solvent purification plant.

Temperature in the preheater, ATFE, and reboiler was controlled by regulating the flow of hot oil through them. The desired pressure in the system was maintained by a high-capacity vacuum pump. Temperature and pressure at key positions were monitored using thermocouples and Pirani gauges. The solvent mixture was pumped through the preheater to remove the moisture present in it. The dehydrated solvent mixture then enters into the ATFE where most of the solvent mixture gets evaporated and remaining portion of the feed was removed as residue which contained degradation products (high boiling point compounds) of the solvent and diluent. In some of the experimental runs, the quantity of the residue was as high as 30% feed which could be either due the inefficient functioning of ATFE or insufficient hot oil flow to evaporate 90–95% of the feed solution. During the course of operation, bottom product from ATFE became dark in color as a result of growing concentration of degradation products of the solvent and partial tarring of TBP. The vapor mixture from the ATFE forms the feed for distillation column where separation of TBP–NPH took place.

The distillation column produced two decontaminated solvent fractions: a distillate (top product) which is pure diluent ($\sim 99\%$ purity) and a concentrate with TBP concentration of about 40–70 vol.%. The data given in Table 4 suggest that top product from the distillation column is almost pure diluent and is suitable for washing aqueous solutions after extraction. It is also observed from the data in Table 4 that C_{12} fraction increased from 19.94% in the feed to 26.14% in the distillate (top product), whereas C_{13} fraction in the feed decreased from 16.2 to 12.74%.

Two types of laboratory tests were carried out to determine the quality of the solvent. In the first test, ruthenium and zirconium retention after several scrubbing with 5 M and 3 M HNO_3 , respectively, were

Table 2
Composition of NPH

$C_{10}H_{22}$ (vol.%)	19.59
$C_{11}H_{24}$ (vol.%)	29.52
$C_{12}H_{26}$ (vol.%)	29.54
$C_{13}H_{28}$ (vol.%)	1.34

Table 3
Operating conditions of a typical experimental run

Equipment	Temperature (°C)	Pressure (torr)
Preheater	120	–
ATFE	131	18
Distillation column (top)	90	3
Reboiler	108	–

Notes: Feed: TBP–NPH mixture with degradation products; feed flow rate: 7.5 L/h; thermo fluid temperature: ~180°C; reflux valve open: 30%.

Table 4
Results of a typical pilot plant run (composition of various streams of distillation column)

Stream	ρ (g/cc)	Composition (%)					
		TBP	NPH	C ₁₀	C ₁₁	C ₁₂	C ₁₃
Feed	0.797	27.19	72.81	15.64	21.03	19.94	16.20
Top product	0.741	0.23	99.70	27.72	33.10	26.14	12.74
Bottom product	0.859	47.34	52.66	2.79	12.06	17.66	20.15

performed. In the second test, phase separation time and interfacial tension measurement with 0.5 M NaOH solution were performed. Table 5 lists the laboratory test results.

It was observed that results differ significantly for ruthenium and zirconium retention, which suggests that the nature of complexing agents is different for ruthenium and zirconium.

5. Conclusion

A pilot plant scale solvent purification system based on vacuum distillation has been designed, developed, and operated successfully. The solvent-recovery system is an integration of different liquid–vapor separation units, such as dehydration column, ATFE, and vacuum distillation column. The performances of the auxiliary equipment were monitored by conducting trial runs with simulated degraded solvent. The purified solvent and diluent obtained from the trial runs were analyzed by measuring the physical and extraction properties. Following conclusions could be drawn from the results of the present investigation:

- The wide difference in boiling point between TBP and diluent is advantageous as only two theoretical stages are sufficient enough to achieve desired separation.

Table 5
Laboratory test results

Parameter	Feed	Bottom product from column
Surface tension (Dynes/cm)	35	26
Phase separation time (s)	~200 (interfacial crud observed)	65–70
Ruthenium-106 retention (mCi/L)	0.102	0.094
Zirconium retention (ppm)	57.53	BDL

- The distillation column produces two decontaminated solvent fractions: a distillate (top product) which is pure diluent (~99% purity) and a concentrate with TBP concentration of about 40–70 vol.% TBP.
- The quality of the products is good for recycling. In fact, the amount of organic generated in extraction process can be reduced considerably by adopting solvent-regeneration process based on vacuum distillation.

Efforts are underway to reduce the rejects volume from ATFE.

Symbols and abbreviations

A	—	heat transfer area, m ²
C_P	—	specific heat, J/g °C
D	—	diameter, m
D_e	—	equivalent diameter, m
F	—	feed rate, mol/hr
h	—	individual heat transfer coefficient, W/m ² K
h_L	—	specific Enthalpy of liquid, J/gmol
h_V	—	specific Enthalpy of vapour, J/gmol
K	—	thermal conductivity, W/m K
L	—	liquid flow rate, mol/h
m	—	mass flow rate, kg/s
N	—	rotational speed, rps
N_b	—	number of blades in the agitator
N_u	—	Nusselt number
R	—	reflux ratio
R_e	—	Reynolds number
Re_f	—	film Reynolds number
Re_r	—	rotational Reynolds number
P	—	pressure, torr
P_r	—	Prandtl number
Q	—	heat load, Watt
q	—	heat transfer rate, watt

q_F	—	quality of feed (liquid fraction in the feed)
T	—	temperature, K
U	—	overall heat transfer coefficient, $W/m^2 K$
V	—	vapour flow rate, mol/h
x	—	liquid phase mole fraction
y	—	vapour phase mole fraction
NPH	—	normal paraffin hydrocarbon
NDD	—	<i>n</i> -dodecane

Greek symbols

ρ	—	density
σ	—	surface tension
μ	—	viscosity
λ	—	latent heat of vaporization

References

- [1] C. Misikas, W. Schulz, J.O. Liljenzin, Solvent extraction in nuclear science and technology, In: J. Rydberg, M. Cox, C. Musika, G. Chopin (Eds.), Solvent Extraction Principles and Practice, 2nd ed., Markel Dekker, New York, 2004, pp. 507–557.
- [2] Z. Nowak, M. Nowak, J. Michalik, A. Owczarczyk, ESR study of irradiated TBP-dodecane- HNO_3 system, Radiochem. Radioanal. Lett. 12 (1972) 2–3.
- [3] C.A. Blake, Jr., Solvent Stability in Nuclear Fuel Reprocessing—evaluation of the literature, Calculation of Radiation Dose and Effects of Iodine and Plutonium, Oak Ridge National Laboratory, Oak Ridge, TN, ORNL-4212, 1968.
- [4] Z. Nowak, Radiative and thermal variations on the dodecane—30% TBP- HNO_3 system, Nukleonika 18 (1973) 447–454.
- [5] S.C. Tripathi, A. Ramanujam, K.K. Gupta, P. Bindu, Studies on the identification of harmful radiolytic products of 30% TBP-dodecane- HNO_3 by gas-chromatography. II. Formation of molecular weight organophosphates, Sep. Sci. Technol. 36 (2001) 2863–2883.
- [6] C. Ginisty, B. Guillaume, Solvent distillation for purex reprocessing plant, Sep. Sci. Technol. 25(13–15) (1990) 1941–1952.
- [7] B.Y. Zilberman, M.N. Makarychev-Mikhailov, V.F. Saprykin, L.B. Shpunt K, S.V. Sakulin, Yu.N. Dulepov, V.V. Glushko, E.N. Semenov, N.A. Mikhailova, V.G. Balakhonov, M.E. Romanov, G.F. Egorov, O.P. Afanas'ev, V.I. Volk, Regeneration of spent TBP-diluent by steam distillation, Radiochemistry 44(3) (2002) 274–281.
- [8] H.J. Clark, G.S. Nichols, Purification of Radioactive Solvent with Flash Vaporizer, USAEC Report DP-849, Savannah River Laboratory, 1965.
- [9] P.R. Auchapt, et al., Solvent Purification using a current of water Vapor, ORNL-tr-244, translation of CEA-R 2404, Plutonium Production Centre at Marcoule, 1964.
- [10] F. Sicilio, T.H. Goodgame, B. Wilkins, Jr., Purification of irradiated tributyl phosphate in kerosene type diluent by distillation, Nucl. Sci. Eng. 9 (1961) 455.
- [11] Y. Kuroda, K. Ogi, Method of Recovery and Regenerating Organic used for the Reprocessing of Radioactive Wastes, Japanese Patent 54-23, 900/A, 1979.
- [12] F. Drain, J.P. Moulin, D. Hugelmann, P. Lukas, Advance Solvent Management in Reprocessing: Five Years of Industrial Experience, ISEC'96, 1996, p. 1789.
- [13] R.H. Perry, D.H. Green, Chemical Engineers Handbook, 7th ed., McGraw Hill, New York, 1997.
- [14] T.R. Bott, J.J.B. Romero, Heat transfer across a scrapped surface, Can. J. Chem. Eng. 41 (1963) 213–219.
- [15] T.R. Bott, M.R. Sheikh, Evaporation at a scraped surface, Chem. Eng. Prog. Symp. Ser. 62(64) (1966) 97–103.